

Effective interpolation of scattered data on a sphere through a Shepard-like method

Zerroudi B.¹, Tayeq H.^{2,3}, El Harrak A.³

¹Laboratory of Engineering Sciences, Faculty of Science, Ibn Zohr University Agadir, Morocco

²SMAD, FPL, Abdelmalek Essaadi University, Tetouan, Morocco

³MMA, FPL, Abdelmalek Essaadi University, Tetouan, Morocco

(Received 20 August 2023; Revised 29 October 2023; Accepted 30 October 2023)

The current paper introduced two approximation operators of large scattered datasets for spherical interpolation. The suggested solution method is an extension of Shepard's well-known method of spherical interpolating, which uses the inverted distances of scattered points as weight functions. With regard to this, the first proposed operator is a linear combination of basis functions with coefficients that are the values of the function. As for the second operator, we consider a spherical triangulation of the scattered points and substitute function values with a local interpolant, which locally interpolates the given data at the vertices of each triangle. Moreover, numerical tests have been carried out to show the interpolation performance, where several numerical results reveal the signified approximation accuracy of the proposed operators.

Keywords: *spherical approximation; spherical RBFs; modified Shepard method; barycentric coordinates.*

2010 MSC: 65D05, 65D15

DOI: 10.23939/mmc2023.04.1174

1. Introduction

Let us consider a half-sphere \mathcal{S} in \mathbb{R}^3 . Let us also suppose that we are given a set of scattered points located on \mathcal{S} , along with real numbers, as the values of the unknown function, associated with each of these points. The cardinal purpose of this paper is to come up with a function defined on \mathcal{S} that interpolates the functional values. The success of this approach is based on many criteria including the cost of producing the interpolant, the robustness of the interpolation process, and the wellness of the interpolant that approximates the underlying function.

This research derives its importance from many scientific fields as geodesy, geography, and computer graphics, numerical weather prediction (NWP), as well as climatology and environmental studies that depend on interpolation procedures (e.g., see [1, 2]).

The problem of constructively defining a smooth surface that interpolates data defined at scattered points in the plane was treated in different ways by several authors, starting from the polynomial approximation, Radial basis functions (RBFs), interpolation by bivariate splines, super-splines. An interesting solution to this problem was introduced by Donald Shepard in the late 1960s, in the famous paper [3]. After that, many studies have studied how to enhance the reproduction quality of the Shepard operator utilizing different forms of weight functions to overcome the disadvantages of the original Shepard method [4, 5] or to increase the reproduction quality of the Shepard operator in the presence of different types of functional and derivative data [6–9].

In concrete problems, the Shepard interpolation method has proven its efficiency and reliability in several works and has applications for the prediction of the dynamical and equilibrium properties of the Born–Oppenheimer potential energy surface of a molecular system [10] and for the use of an inverse problem of residual fields [11]. But those applications and studies are presented in Euclidean spaces, with regard to the spherical interpolation problem, many methods have been proposed to solve the spherical interpolation problem for scattered data. In fact, it would take extensive effort

to compile a list of the various methods which have been proposed for this problem. Some of these methods include Spherical harmonics, Spherical analogs of thin plate splines, tensor splines, radial basis functions [12–20] among others).

Shepard method has proven to be a powerful tool for analyzing scattered data on \mathbb{R}^n . In this paper, the basic idea is to extend to the sphere the Shepard and triangular Shepard method (see [6, 21]) for the interpolation of large scattered and track data sets in bi-dimensional domains. Where, we consider an extended version of the Shepard methods in the sphere in \mathbb{R}^3 . In fact, we preserve all the advantages of the Shepherd method, in which the interpolant is directly expressed as a linear combination of basis functions which depend on the geodesic distance. Also, the basis functions have many important properties such as its derivative equal to zero at the interpolation points. We refer to the fact that we rely on two types of basis functions. The first one is the point basis functions, which the coefficients of the linear combination in this case are values of the unknown function. As for the second type of basis functions, they are the triangular basis functions; the coefficients of the linear combination, in this case, are local interpolants over a triangle. The results proven in this paper can be used in several fields, especially when modeling a concrete sphere such as maritime traffic, GPS satellites, and any problem that requires good precision interpolation of 3D positions [22].

This paper is organized as follows. In Section 2, we present the interpolation problem on the sphere and introduce the interpolant which is based on a suitable class of cardinal basis functions that depend only on geodesic distances on the sphere. In Section 3, we give the basis function based on triangulation and present a local interpolant over each spherical triangle. Using the linear combination of triangular basis functions and a local interpolant, we present the global operator on the sphere. In Section 4, we discuss numerical tests on the unit sphere, which demonstrate the accuracy and the fastness of such operators and confirm the theoretical results.

2. Spherical Shepard's method

In this paper, we note by \mathcal{S} a half-sphere in \mathbb{R}^3 of radius R and $\Omega = \{\mathbf{u} = (u_1, u_2, u_3) \in \mathbb{R}^3\} \subset \mathcal{S}$ is an open set. Given a set $X_n = \{\mathbf{u}_1, \dots, \mathbf{u}_n\}$ of distinct data points arbitrarily distributed on Ω , associated with the corresponding set $F_n = \{f_1, \dots, f_n\}$ of data values of an unknown function $f: \Omega \rightarrow \mathbb{R}$. We are interested in this paper on finding a (continuous) function $F[f]: \Omega \rightarrow \mathbb{R}$, which satisfies the interpolation conditions

$$F[f](\mathbf{u}_i) = f_i, \quad i = 1, \dots, n. \quad (1)$$

It should be mentioned that for constructing an approximation operator that verifies Equation 1, a slight change in notation was desirable for the classical Shepard operator [6]. In fact, we can consider specializing the Shepard method to the sphere by considering an interpolant of the form

$$S_\mu[f](\mathbf{u}) = \sum_{i=1}^n A_{\mu,i}(\mathbf{u}) f_i, \quad \mathbf{u} \in \Omega. \quad (2)$$

This interpolant uses point-based basis functions

$$A_{\mu,i}(\mathbf{u}) = \frac{(d_g(\mathbf{u}, \mathbf{u}_i))^{-\mu}}{\sum_{k=1}^n (d_g(\mathbf{u}, \mathbf{u}_k))^{-\mu}}, \quad i = 1, \dots, n, \quad (3)$$

where μ is a real positive parameter control and $d_g(\mathbf{u}, \mathbf{u}_i)$ denotes the geodesic distance, i.e. the length of the (shorter) part of the great circle joining \mathbf{u} and \mathbf{u}_i and μ is a real positive parameter control. The weight functions $A_{\mu,i}(\mathbf{u})$, $i = 1, \dots, n$, are cardinal basis functions; they satisfy for all $\mathbf{u} \in \mathcal{S}$ and any $i, j = 1, \dots, n$, the conditions

$$A_{\mu,i}(\mathbf{u}) \geq 0, \quad \sum_{i=1}^n A_{\mu,i}(\mathbf{u}) = 1, \quad A_{\mu,i}(\mathbf{u}_j) = \delta_{ij},$$

where δ_{ij} is the Kronecker delta.

Proposition 5. The operator S_μ verifies the interpolation properties; i.e. for all $i = 1, \dots, n$, we have

$$S_\mu[f](\mathbf{u}_i) = f(\mathbf{u}_i).$$

Proof. Let $\mathbf{u}_i \in X_n, i = 1, \dots, n$, by using the Lagrange properties verify by the basis functions $A_{\mu,i}(\mathbf{u})$, we can verify easily that

$$S_\mu[f](\mathbf{u}_i) = f(\mathbf{u}_i).$$

■

3. Spherical-triangle Shepard's method

In order to extend the triangular Shepard operator in the planer [21] to the sphere, we need to construct spherical barycentric coordinates. Analogous to classical planar barycentric coordinates that describe the positions of points in a plane with respect to the vertices of a given planar triangle, spherical barycentric coordinates describe the positions of points on a sphere with respect to the vertices of a given spherical triangle.

Definition 1. A **spherical triangle** t consists of a set of distinct vertices v_1, v_2, v_3 located on a sphere and a set of arcs $(v_i; v_j)$ that connect the vertices v_i and v_j by geodesic lines (these are the arcs of great circles on the sphere) (see Figure 1).

Definition 2. Let t be a **spherical triangle** on a sphere \mathcal{S} , with vertices $\mathbf{u}_1, \mathbf{u}_2, \mathbf{u}_3$. We call any values ϕ_1, ϕ_2, ϕ_3 , spherical barycentric coordinates respect to t , if they satisfy

$$\sum_{i=1}^3 \phi_i(\mathbf{u}) \mathbf{u}_i = \mathbf{u} \quad \forall \mathbf{u} \in \mathcal{S}. \tag{4}$$

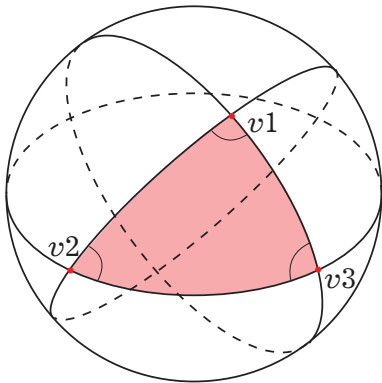


Fig. 1. A spherical triangle.

To show how barycentric coordinates can be defined for an arbitrary triangle on a sphere, consider a spherical triangle t on the unit sphere centered at the origin \mathcal{S}_O , with vertices $\mathbf{u}_1, \mathbf{u}_2, \mathbf{u}_3$. Let \mathbf{u} be a point on the sphere, such that the angle between \mathbf{u} and \mathbf{u}_i different to $\pm \frac{\pi}{2}$, and for $i = 1, 2, 3$, let \mathbf{u}'_i be the intersection point of the line $(O\mathbf{u}_i)$, passing by O (origin) and \mathbf{u}_i , and the tangent plane $T_{\mathbf{u}}$ at \mathbf{u} to the sphere \mathcal{S}_O (the map $\mathbf{u}_i \rightarrow \mathbf{u}'_i$ is a gnomonic projection [23]). The vertices $\mathbf{u}'_1, \mathbf{u}'_2$ and \mathbf{u}'_3 define a triangle t' in the plane $T_{\mathbf{u}}$. Now, we can evaluate the planar barycentric coordinates $\lambda_i, i = 1, 2, 3$ of \mathbf{u} with respect to the triangle $t' = [\mathbf{u}'_1, \mathbf{u}'_2, \mathbf{u}'_3]$. Therefore, as a choice of λ_i , we can set [24]

$$\lambda_1(\mathbf{u}) = \frac{A(\mathbf{u}, \mathbf{u}'_2, \mathbf{u}'_3)}{A(\mathbf{u}'_1, \mathbf{u}'_2, \mathbf{u}'_3)}, \quad \lambda_2(\mathbf{u}) = \frac{A(\mathbf{u}'_1, \mathbf{u}, \mathbf{u}'_3)}{A(\mathbf{u}'_1, \mathbf{u}'_2, \mathbf{u}'_3)}, \quad \lambda_3(\mathbf{u}) = \frac{A(\mathbf{u}'_1, \mathbf{u}'_2, \mathbf{u})}{A(\mathbf{u}'_1, \mathbf{u}'_2, \mathbf{u}'_3)},$$

where $A(\mathbf{u}, \mathbf{v}, \mathbf{w})$ denote the signed area of the planar triangle $[\mathbf{u}, \mathbf{v}, \mathbf{w}]$. Consequently, the functions $\lambda_i(\mathbf{u}), i = 1, 2, 3$, satisfy the following properties

$$\lambda_i(\mathbf{u}'_k) = \delta_{ik} \quad i, k = 1, 2, 3, \tag{5}$$

$$\sum_{i=1}^3 \lambda_i(\mathbf{u}) = 1 \quad \forall \mathbf{u} \in T_{\mathbf{u}}, \tag{6}$$

$$\sum_{i=1}^3 \lambda_i(\mathbf{u}) \mathbf{u}'_i = \mathbf{u} \quad \forall \mathbf{u} \in T_{\mathbf{u}}. \tag{7}$$

Proposition 6. Spherical barycentric coordinates $\phi_i(\mathbf{u})$, $i = 1, 2, 3$, of \mathbf{u} respect to spherical triangle $t = [\mathbf{u}_1, \mathbf{u}_2, \mathbf{u}_3]$ that satisfy the linear precision property (4), given by

$$\phi_i(\mathbf{u}) := \lambda_i(\mathbf{u}) \langle \mathbf{u}'_i, \mathbf{u}_i \rangle, \tag{8}$$

where $\langle \cdot, \cdot \rangle$ is the usual scalar product in \mathbb{R}^3 .

Proof. By the construction of points \mathbf{u}'_i , $i = 1, 2, 3$, we can write $\mathbf{u}'_i = \langle \mathbf{u}'_i, \mathbf{u}_i \rangle \mathbf{u}_i$, $i = 1, 2, 3$. By the equation (7), we have

$$\sum_{i=1}^3 \lambda_i(\mathbf{u}) \langle \mathbf{u}'_i, \mathbf{u}_i \rangle \mathbf{u}_i = \mathbf{u} \quad \forall \mathbf{u} \in T_{\mathbf{u}},$$

by taking $\phi_i(\mathbf{u}) = \lambda_i(\mathbf{u}) \langle \mathbf{u}'_i, \mathbf{u}_i \rangle$, the equation (4) yields. ■

Remark 1. (1) The definition of $\phi_i(\mathbf{u})$, $i = 1, 2, 3$, can be extended continuously to the case if the angle between \mathbf{u} and \mathbf{u}_i approaches $\pm \frac{\pi}{2}$. (2) The spherical barycentric coordinates $\phi_i(\mathbf{u})$, $i = 1, 2, 3$, satisfy the interpolation property; $\phi_i(\mathbf{u}_k) = \delta_{ik}$.

In [25], it was pointed out that partition of unity (6) and linear precision (7) contradict each other on spheres. In fact, for \mathbf{u} inside the triangle we have

$$\sum_{i=1}^3 \phi_i(\mathbf{u}) \geq 1.$$

Lemma 1. Let $t = [\mathbf{u}_1, \mathbf{u}_2, \mathbf{u}_3]$ be a spherical triangle located on the sphere $\mathcal{S}_{\mathcal{O}}$ such as $dg(\mathbf{u}_i, \mathbf{u}_j) < \frac{\pi}{2}$, $i, j = 1, 2, 3$, (the angle between \mathbf{u}_i and \mathbf{u}_j less than $\frac{\pi}{2}$). For any \mathbf{u} inside t , we have

$$0 \leq \sum_{i=1}^3 \phi_i(\mathbf{u}) - 1 \leq \frac{h_t^2}{2 \cos(h_t)},$$

where $h_t = \max(dg(\mathbf{u}_1, \mathbf{u}_2), dg(\mathbf{u}_1, \mathbf{u}_3), dg(\mathbf{u}_3, \mathbf{u}_2))$.

Proof. Let \mathbf{u} inside the spherical triangle t , by the Proposition 6

$$\sum_{i=1}^3 \phi_i(\mathbf{u}) - 1 = \sum_{i=1}^3 \lambda_i(\mathbf{u}) \langle \mathbf{u}'_i, \mathbf{u}_i \rangle - 1 = \sum_{i=1}^3 \lambda_i(\mathbf{u}) (\langle \mathbf{u}'_i, \mathbf{u}_i \rangle - 1). \tag{9}$$

Note that $\langle \mathbf{u}'_i, \mathbf{u}_i \rangle = \|\mathbf{u}'_i\|$ ($\|\cdot\|$ is the Euclidean norm); inasmuch as the angle between \mathbf{u}_i and \mathbf{u} less than $\frac{\pi}{2}$. The geodesic distance of the points \mathbf{u}_i and \mathbf{u} of the unit sphere $\mathcal{S}_{\mathcal{O}}$, is

$$dg(\mathbf{u}_i, \mathbf{u}) = \arccos(\langle \mathbf{u}_i, \mathbf{u} \rangle).$$

On the other hand, we have $\langle \mathbf{u}'_i, \mathbf{u} \rangle = \langle \mathbf{u}_i, \mathbf{u} \rangle \|\mathbf{u}'_i\| = \cos(dg(\mathbf{u}_i, \mathbf{u})) \|\mathbf{u}'_i\|$. Since \mathbf{u} and $\mathbf{u} - \mathbf{u}'_i$ are orthogonal in \mathbf{u} , we find that $\langle \mathbf{u}'_i, \mathbf{u} \rangle = 1$, and so we get

$$\|\mathbf{u}'_i\| = \frac{1}{\cos(dg(\mathbf{u}_i, \mathbf{u}))},$$

from it we conclude

$$\|\mathbf{u}'_i\| - 1 = \frac{1 - \cos(dg(\mathbf{u}_i, \mathbf{u}))}{\cos(dg(\mathbf{u}_i, \mathbf{u}))}.$$

By using the inequality $1 - \cos(r) \leq \frac{r^2}{2}$ for any $r \geq 0$, and the fact that $dg(\mathbf{u}_i, \mathbf{u}) \leq h_t < \frac{\pi}{2}$, we obtain

$$|\|\mathbf{u}'_i\| - 1| \leq \frac{h_t^2}{2 \cos(h_t)}. \tag{10}$$

Finally, by using $\sum_{i=1}^3 \lambda_i(\mathbf{u}) = 1$, (9) and (10), we gain

$$\left| \sum_{i=1}^3 \phi_i(\mathbf{u}) - 1 \right| \leq \frac{h_t^2}{2 \cos(h_t)}.$$

■

To extend the point-based basis functions in (3) to spherical-triangle-based basis functions, let us consider a triangulation $T = \{t_1, \dots, t_m\}$ of the nodes X_n and we suppose that the distance between any two distinct points of X_n is not more than $\frac{\pi}{2}R$, with R being the radius of the sphere \mathcal{S} . That is, each $t_j = [\mathbf{u}_{j_1}, \mathbf{u}_{j_2}, \mathbf{u}_{j_3}]$ is a spherical triangle with vertices in X_n and each node \mathbf{u}_i is the vertex of at least one triangle, hence

$$\cup_j \{j_1, j_2, j_3\} = \{1, 2, \dots, n\}.$$

We note that the triangulation set T can be the *Delaunay triangulation* of X_n , or it can be a general triangulation with overlapping or disjoint triangles.

The basis functions corresponding to the Spherical-triangulation T are then defined by

$$\Phi_{\mu,j}(\mathbf{u}) = \frac{\prod_{\ell=1}^3 \frac{1}{(d_g(\mathbf{u}, \mathbf{u}_{j_\ell}))^\mu}}{\sum_{k=1}^m \prod_{\ell=1}^3 \frac{1}{(d_g(\mathbf{u}, \mathbf{u}_{k_\ell}))^\mu}} = \frac{\prod_{k \neq j} \prod_{\ell=1}^3 (d_g(\mathbf{u}, \mathbf{u}_{k_\ell}))^\mu}{\sum_{k=1}^m \prod_{i \neq k} \prod_{\ell=1}^3 (d_g(\mathbf{u}, \mathbf{u}_{i_\ell}))^\mu}, \quad j = 1, \dots, m. \tag{11}$$

The basis functions $\Phi_{\mu,j}$ (11) are continuous, non-negative and form a partition of unity, i.e.,

$$\Phi_{\mu,j}(\mathbf{u}) \geq 0, \quad \sum_{j=1}^n \Phi_{\mu,j}(\mathbf{u}) = 1,$$

also, they satisfy the following properties.

Proposition 7. The spherical triangle-based basis function in (11) disappears at all nodes $\mathbf{u}_i \in X_n$ that are not a vertex of the corresponding spherical triangle t_j , i.e., $\Phi_{\mu,j}(\mathbf{u}_i) = 0$, for any $j = 1, \dots, m$ and $i \notin \{j_1, j_2, j_3\}$.

Proof. Let $\mathbf{u}_i \in X_n$ and $j \in \{1, \dots, m\}$, $i \notin \{j_1, j_2, j_3\}$. Let us consider J_i the set of indices of all spherical triangles that have \mathbf{u}_i as a vertex ($J_i = \{k \in \{1, \dots, m\}; i \in \{k_1, k_2, k_3\}\}$). Then, $\Phi_{\mu,j}$ becomes as

$$\Phi_{\mu,j}(\mathbf{u}) = \frac{\prod_{\ell=1}^3 \frac{1}{(d_g(\mathbf{u}, \mathbf{u}_{j_\ell}))^\mu}}{\sum_{k \in J_i} \prod_{\ell=1}^3 \frac{1}{(d_g(\mathbf{u}, \mathbf{u}_{k_\ell}))^\mu} + \sum_{k \notin J_i} \prod_{\ell=1}^3 \frac{1}{(d_g(\mathbf{u}, \mathbf{u}_{k_\ell}))^\mu}},$$

by multiplying both the numerator and the denominator of this equation with $(d_g(\mathbf{u}, \mathbf{u}_i))^\mu$, then

$$\Phi_{\mu,j}(\mathbf{u}) = \frac{\prod_{\ell=1}^3 \frac{(d_g(\mathbf{u}, \mathbf{u}_i))^\mu}{(d_g(\mathbf{u}, \mathbf{u}_{j_\ell}))^\mu}}{\sum_{k \in J_i} \prod_{\ell=1, \ell \neq i}^3 \frac{1}{(d_g(\mathbf{u}, \mathbf{u}_{k_\ell}))^\mu} + \sum_{k \notin J_i} \prod_{\ell=1}^3 \frac{(d_g(\mathbf{u}, \mathbf{u}_i))^\mu}{(d_g(\mathbf{u}, \mathbf{u}_{k_\ell}))^\mu}},$$

by noticing that $\prod_{\ell=1}^3 \frac{(d_g(\mathbf{u}, \mathbf{u}_i))^\mu}{(d_g(\mathbf{u}, \mathbf{u}_{j_\ell}))^\mu}$ vanish at \mathbf{u}_i , we conclude that $\Phi_{\mu,j}(\mathbf{u}_i) = 0$. ■

As an immediate consequence of the partition of unity property and the last proposition, we obtain the following remark.

Remark 2. For any $\mathbf{u}_i \in X_n$, we have

$$\sum_{j \in J_i} \Phi_{\mu,j}(\mathbf{u}_i) = 1. \tag{12}$$

Now, we define the approximation operator that locally interpolates the given data at the vertices of each triangle. For $t_j \in T$, this operator $P_j[f]: \Omega \rightarrow \mathbb{R}$ can be written as

$$P_j[f](\mathbf{u}) = \sum_{\ell=1}^3 \phi_{j,j_\ell}(\mathbf{u}) f_{j_\ell}, \tag{13}$$

where $f_{j_\ell} := f(\mathbf{u}_{j_\ell})$ and the basis $\phi_{j,j_\ell}(\mathbf{u})$, $\ell = 1, 2, 3$, are the spherical barycentric coordinates of \mathbf{u} (Proposition 6) with respect to the spherical triangle $t_j = [\mathbf{u}_{j_1}, \mathbf{u}_{j_2}, \mathbf{u}_{j_3}]$, for all $j \in \{1, \dots, m\}$.

Proposition 8. For any $j = 1, \dots, m$, the polynomial $P_j[f](\mathbf{u})$ on t_j

- (1) depends symmetrically on three vertices of t_j ,
- (2) interpolates functional evaluations at the vertices of t_j ,
- (3) $P_j[f] = f$ if f is a linear function.

Proof.

(1) As an immediate consequence of the construction of $P_j[f](\mathbf{u})$ (13), the first propriety yields.

(2) If \mathbf{u}_{j_i} is a vertex of the triangle $t_j = [\mathbf{u}_{j_1}, \mathbf{u}_{j_2}, \mathbf{u}_{j_3}]$, then $\phi_{j,j_\ell}(\mathbf{u}_{j_i}) = \delta_{i\ell}$, as a consequence $P_j[f](\mathbf{u}_{j_i}) = f_{j_i}$.

(3) Let f be a linear function, according to the linear precision property verify by $\phi_{j,j_\ell}(\mathbf{u})$, we have

$$f(\mathbf{u}) = f\left(\sum_{\ell=1}^3 \phi_{j,j_\ell}(\mathbf{u}) \mathbf{u}_{j_\ell}\right) = \sum_{\ell=1}^3 \phi_{j,j_\ell}(\mathbf{u}) f(\mathbf{u}_{j_\ell}),$$

then, $P_j[f] = f$. ■

Let us now assume that $f \in C^k(\Omega)$ and introduce the semi-norm

$$|D^k f|_\Omega = \sup_{\mathbf{u} \in \Omega} \sup \{|D_{\mathbf{y}}^k f(\mathbf{u})|; \mathbf{y} \in \mathbb{R}^3, \|\mathbf{y}\| = 1\},$$

where $D_{\mathbf{y}}^k f(\mathbf{u})$ is the k -th directional derivative. For any $\mathbf{u} \in \Omega$ and $\mathbf{y} \in \mathbb{R}^3$, we have

$$|D_{\mathbf{y}}^k f(\mathbf{u})| \leq |D^k f|_\Omega \|\mathbf{y}\|.$$

Proposition 9. Let $f \in C^2(\Omega)$, then for each $\mathbf{u} \in t_j = [\mathbf{u}_{j_1}, \mathbf{u}_{j_2}, \mathbf{u}_{j_3}]$, $j = 1, \dots, m$, we have

$$|P_j[f](\mathbf{u}) - f(\mathbf{u})| \leq \frac{h_{t_j}^2}{2 \cos(h_{t_j})} (|f(\mathbf{u}_{j_1}) - \langle \mathbf{u}_{j_1}, \nabla f(\mathbf{u}_{j_1}) \rangle| + |D^2 f|_\Omega) + \frac{|D^2 f|_\Omega d_g(\mathbf{u}, \mathbf{u}_{j_1})}{2},$$

where $h_{t_j} = \max\{d_g(\mathbf{u}_{j_1}, \mathbf{u}_{j_2}), d_g(\mathbf{u}_{j_1}, \mathbf{u}_{j_3}), d_g(\mathbf{u}_{j_2}, \mathbf{u}_{j_3})\}$.

Proof. For any $j = 1, \dots, m$ and $\ell = 2, 3$, we expand $f(\mathbf{u}_\ell)$ in truncated Taylor series centered at \mathbf{u}_1 [26], we obtain

$$f(\mathbf{u}_\ell) = f(\mathbf{u}_{j_1}) + D_{\mathbf{u}_{j_\ell} - \mathbf{u}_{j_1}} f(\mathbf{u}_{j_1}) + R[f, \mathbf{u}_{j_1}](\mathbf{u}_{j_\ell}), \tag{14}$$

where $R[f, \mathbf{u}_{j_1}]$ is the remainder term in the first order Taylor expansion of f at \mathbf{u}_{j_1} . By substituting (14) in (13) and using (4), for any $\mathbf{u} \in t_j$ we gain

$$\begin{aligned} P_j[f](\mathbf{u}) &= \sum_{\ell=1}^3 \phi_{j,j_\ell}(\mathbf{u}) f_{j_\ell} + D_{\mathbf{u} - \mathbf{u}_{j_1}} f(\mathbf{u}_{j_1}) - \left(\sum_{\ell=1}^3 \phi_{j,j_\ell}(\mathbf{u}) - 1\right) D_{\mathbf{u}_{j_1}} f(\mathbf{u}_{j_1}) \\ &\quad + \phi_{j,j_2}(\mathbf{u}) R[f, \mathbf{u}_{j_1}](\mathbf{u}_{j_2}) + \phi_{j,j_3}(\mathbf{u}) R[f, \mathbf{u}_{j_1}](\mathbf{u}_{j_3}) \\ &= f(\mathbf{u}_{j_1}) + D_{\mathbf{u} - \mathbf{u}_{j_1}} f(\mathbf{u}_{j_1}) + (f_{j_1} - D_{\mathbf{u}_{j_1}} f(\mathbf{u}_{j_1})) \left(\sum_{\ell=1}^3 \phi_{j,j_\ell}(\mathbf{u}) - 1\right) \\ &\quad + \phi_{j,j_2}(\mathbf{u}) R[f, \mathbf{u}_{j_1}](\mathbf{u}_{j_2}) + \phi_{j,j_3}(\mathbf{u}) R[f, \mathbf{u}_{j_1}](\mathbf{u}_{j_3}). \end{aligned}$$

Therefore, by noticing that $f(\mathbf{u}_{j_1}) + D_{\mathbf{u} - \mathbf{u}_{j_1}} f(\mathbf{u}_{j_1})$ is the first order Taylor polynomial $T_1[f, \mathbf{u}_{j_1}]$ of f at \mathbf{u}_{j_1} , we find

$$\begin{aligned} P_j[f](\mathbf{u}) - f(\mathbf{u}) &= (T_1[f, \mathbf{u}_{j_1}](\mathbf{u}) - f(\mathbf{u})) + (f_{j_1} - D_{\mathbf{u}_{j_1}} f(\mathbf{u}_{j_1})) \left(\sum_{\ell=1}^3 \phi_{j,j_\ell}(\mathbf{u}) - 1\right) \\ &\quad + \phi_{j,j_2}(\mathbf{u}) R[f, \mathbf{u}_{j_1}](\mathbf{u}_{j_2}) + \phi_{j,j_3}(\mathbf{u}) R[f, \mathbf{u}_{j_1}](\mathbf{u}_{j_3}). \end{aligned}$$

Firstly, the remainder term $R[f, \mathbf{v}](\mathbf{u})$ bounded in standard way

$$|R[f, \mathbf{v}](\mathbf{u})| \leq \frac{|D^2 f|_\Omega \|\mathbf{u} - \mathbf{v}\|^2}{2} \leq \frac{|D^2 f|_\Omega d_g(\mathbf{u}, \mathbf{v})^2}{2},$$

then

$$|R[f, \mathbf{u}_{j_1}](\mathbf{u}_{j_2})| \leq \frac{|D^2 f|_\Omega h_{t_j}^2}{2}, \quad |R[f, \mathbf{u}_{j_1}](\mathbf{u}_{j_3})| \leq \frac{|D^2 f|_\Omega h_{t_j}^2}{2},$$

and

$$|T_1[f, \mathbf{u}_{j_1}](\mathbf{u}) - f(\mathbf{u})| = |R[f, \mathbf{u}_{j_1}](\mathbf{u})| \leq \frac{|D^2 f|_\Omega d_g(\mathbf{u}, \mathbf{u}_{j_1})^2}{2}.$$

On the other hand, by using (9), we obtain

$$|P_j[f](\mathbf{u}) - f(\mathbf{u})| \leq \frac{|D^2 f|_{\Omega} d_g(\mathbf{u}, \mathbf{u}_{j_1})^2}{2} + \frac{|f_{j_1} - D_{\mathbf{u}_{j_1}} f(\mathbf{u}_{j_1})| h_{t_j}^2}{2 \cos(h_{t_j})} + \frac{|D^2 f|_{\Omega} h_{t_j}^2}{2} (\phi_{j,j_2}(\mathbf{u}) + \phi_{j,j_3}(\mathbf{u})), \tag{15}$$

that is because $\phi_{j,j_\ell}(\mathbf{u})$, $\ell = 1, 2, 3$, are positive if \mathbf{u} inside t_j . According to Proposition 6, we have $\phi_{j,j_2}(\mathbf{u}) + \phi_{j,j_3}(\mathbf{u}) = \lambda_{j,j_2}(\mathbf{u}) \|\mathbf{u}'_{j_2}\| + \lambda_{j,j_3}(\mathbf{u}) \|\mathbf{u}'_{j_3}\|$, and from the above

$$\phi_{j,j_2}(\mathbf{u}) + \phi_{j,j_3}(\mathbf{u}) = \lambda_{j,j_2}(\mathbf{u}) \frac{1}{\cos(dg(\mathbf{u}_{j_2}, \mathbf{u}))} + \lambda_{j,j_3}(\mathbf{u}) \frac{1}{\cos(dg(\mathbf{u}_{j_3}, \mathbf{u}))},$$

then, for any \mathbf{u} inside t_j , we have

$$\phi_{j,j_2}(\mathbf{u}) + \phi_{j,j_3}(\mathbf{u}) \leq \frac{1}{\cos(h_{t_j})}.$$

Now, by substituting the last equation into (15), we find the answer which was to be demonstrated. ■

By combining the spherical triangle-based basis functions (11) with the local operators $P_j[f](\mathbf{u})$ (13), and for any $\mu > 0$ the triangular spherical Shepard operator is defined by

$$K_\mu[f](\mathbf{u}) = \sum_{j=1}^m \Phi_{\mu,j}(\mathbf{u}) P_j[f](\mathbf{u}). \tag{16}$$

Theorem 1. *The operator K_μ (16)*

(1) *interpolate the function data at each \mathbf{u}_i , $i = 1, \dots, n$, that is,*

$$K_\mu[f](\mathbf{u}_i) = f_i, \quad i = 1, \dots, n;$$

(2) *reproduce all linear function, that is, if f is a linear function, we have*

$$K_\mu[f] = f.$$

Proof.

(1) Let \mathbf{u}_i be a vertex. By evaluating in (16), we have

$$K_\mu[f](\mathbf{u}_i) = \sum_{j=1}^m \Phi_{\mu,j}(\mathbf{u}_i) P_j[f](\mathbf{u}_i) = \sum_{j \in J_i} \Phi_{\mu,j}(\mathbf{u}_i) P_j[f](\mathbf{u}_i) + \sum_{j \notin J_i} \Phi_{\mu,j}(\mathbf{u}_i) P_j[f](\mathbf{u}_i),$$

by the Proposition 8, we have $P_j[f](\mathbf{u}_i) = f_i$ if \mathbf{u}_i a vertex of a triangle t_j (i.e. $i \in \{j_1, j_2, j_3\}$). On the other hand, if \mathbf{u}_i is not a vertex of a triangle t_j , we have $\Phi_{\mu,j}(\mathbf{u}_i) = 0$. Therefore we can conclude

$$K_\mu[f](\mathbf{u}_i) = f_i \sum_{j \in J_i} \Phi_{\mu,j}(\mathbf{u}_i),$$

finally by using the result $\sum_{j \in J_i} \Phi_{\mu,j}(\mathbf{u}_i) = 1$, we obtain the interpolation property of $K_\mu[f]$.

(2) Show that $K_\mu[f]$ reproduces all linear functions. Let us consider f a linear function, by Proposition 8 we have $P_j[f] = f$, $j = 1, \dots, m$, so

$$K_\mu[f](\mathbf{u}) = \sum_{j=1}^m \Phi_{\mu,j}(\mathbf{u}) f(\mathbf{u}).$$

Now, by using the partition of unity property of $\Phi_{\mu,j}(\mathbf{u})$, we find that $K_\mu[f]$ reproduces all linear functions. ■

4. Numerical results

In this section, we present numerical results for the operators S_μ and K_μ using scattered data on the sphere. Indeed, this investigation gives a numerical validation of the theoretical results of the operators applied to the sphere.

We carried out our various numerical experiments with n Halton scattered data points denoted by X_n on the unit spherical part of $\mathcal{S}_\mathcal{O}$ ($x \geq 0, y \geq 0, z \geq 0$) (see Figure 2), and 12 test functions. The first 6 test functions were introduced in [27] and the last 6 ones by various authors [5, 8, 28–30]. The 12 functions are given by:

Exponential:

$$f_1(x, y, z) = 0.75 \exp\left(-\frac{(9x-2)^2 + (9y-2)^2 + (9z-2)^2}{4}\right) + 0.50 \exp\left(-\frac{(9x-7)^2 + (9y-3)^2 + (9z-7)^2}{4}\right) + 0.75 \exp\left(-\frac{(9x+1)^2}{49} - \frac{(9y+1)^2}{10} - \frac{(9z+1)^2}{10}\right) - 0.20 \exp\left(- (9x-1)^2 - (9y-7)^2 - (9z-7)^2\right);$$

Ccliff:

$$f_2(x, y, z) = \frac{\tanh(9z - 9y - 9x) + 1}{9};$$

Saddle:

$$f_3(x, y, z) = \frac{(1.25 + \cos(5.4y)) \cos(6z)}{(6 + 6(3x - 1)^2)};$$

Steep:

$$f_4(x, y, z) = \frac{1}{3} \exp\left(\left(-\frac{81}{4}\right) \left((x-0.5)^2 + (y-0.5)^2 + (z-0.5)^2\right)\right);$$

Sphere:

$$f_5(x, y, z) = \frac{\sqrt{64 - 81((x-0.5)^2 + (y-0.5)^2 + (z-0.5)^2)}}{9} - 0.5;$$

Gentle:

$$f_6(x, y, z) = \frac{1}{3} \exp\left(-\frac{81}{16} \left((x-0.5)^2 + (y-0.5)^2 + (z-0.5)^2\right)\right);$$

$$f_7(x, y, z) = 0.1(\exp(x) + \exp(y + z));$$

$$f_8(x, y, z) = 2 \cos(10x) \sin(10y) + \sin(10xyz);$$

$$f_9(x, y, z) = \exp\left(-\frac{(5-10x)^2}{2}\right) + 0.75 \exp\left(-\frac{(5-10y)^2}{2}\right) + 0.75 \exp\left(-\frac{(5-10z)^2}{2}\right);$$

$$+ 0.75 \exp\left(-\frac{(5-10x)^2}{2}\right) \exp\left(-\frac{(5-10y)^2}{2}\right) \exp\left(-\frac{(5-10z)^2}{2}\right);$$

$$f_{10}(x, y, z) = \exp\left(-0.04\sqrt{(80x-40)^2 + (90y-45)^2 + (90z-45)^2}\right) \times \cos\left(0.15\sqrt{(80x-40)^2 + (90y-45)^2 + (90z-45)^2}\right);$$

$$f_{11}(x, y, z) = \frac{1}{2} \sin(2\pi x) \cos(2\pi y) \cos(2\pi z);$$

$$f_{12}(x, y, z) = \frac{(2x-1)(1-2y)(1-2z)+1}{2}.$$

Furthermore, to test and verify the effectiveness of approximation operator K_μ , we use five sets of quasi-uniformly distributed points, in order to generate two types of triangulations, namely Delaunay triangulation and Compact one.

Finally, to study accuracy of the operators S_μ and K_μ , we compute the maximum absolute error e_{\max} , the average error e_{mean} , and the mean square error e_{MS} given by

$$e_{\max} = \max_{1 \leq i \leq n_e} e_i, \quad e_{\text{mean}} = \frac{1}{n_e} \sum_{i=1}^{n_e} e_i, \quad e_{\text{MS}} = \sqrt{\frac{\sum_{i=1}^{n_e} e_i^2}{n_e}}, \quad (17)$$

where e_i are the pointwise errors computed in absolute value at n_e evaluation points. For each f of 12 test functions, we construct $S_\mu[f]$ and $K_\mu[f]$, calculate e_i at the points of a quasi-regular grid and evaluate the errors; maximum, average, and mean square (17).

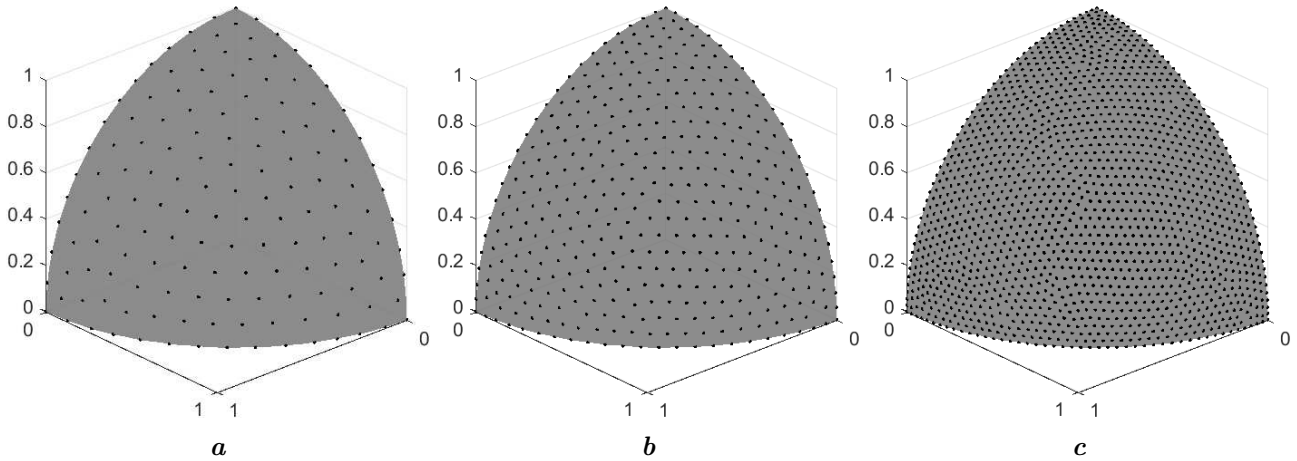


Fig. 2. Three of the five sets of points using: 146 points (a), 396 points (b), and 1512 points (c).

Now, we consider five sets of quasi-uniformly distributed points on \mathcal{S}_O . In Table 1, we resume five sets and the corresponding Delaunay triangulation (see Figure 3), and in Table 2 the Compact triangulation (see Figure 4).

Table 1. Generated Delaunay triangulation with n points, m triangles and maximum edge length h_{max} .

mesh	n	m	h_{max}
1	146	249	1.894294e-01
2	396	721	1.137478e-01
3	1512	2884	5.690042e-02
4	5907	11536	2.845354e-02
5	23349	46144	1.422718e-02

Table 2. Generated Compact triangulation with n points, m triangles and maximum edge h_{max} .

mesh	n	m	h_{max}
1	146	80	2.523751e-01
2	396	209	1.355948e-01
3	1512	810	6.824603e-02
4	5907	3130	3.486799e-02
5	23349	12079	1.760677e-02

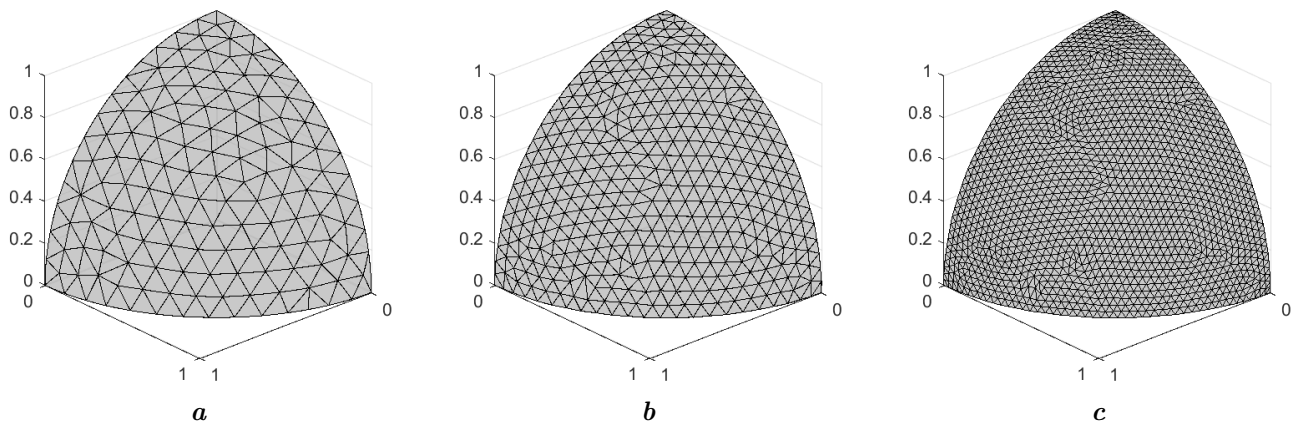


Fig. 3. Three of five Delaunay triangulations using: 146 points (a), 396 points (b), and 1512 points (c), corresponding to the three sets of Figure 2.

We construct the operators $S_2[f_i]$ and $K_2[f_i]$ for each test function f_i , $i = 1, \dots, 12$. Then we calculate the errors (17) at 184576 evaluation points. Figure 5 shows the approximation error with respect to the maximum edge length h_{max} , where the plots are given in logarithmic scale of the approximation error with respect to the maximum edge length h_{max} .

Now, we carried out an experiment to show the approximation accuracies of the operators S_2 and K_2 , where we apply those operators to 12 test functions using 1119 Halton points (see Figure 6-a). Concerning K_2 , we consider two types of triangulation, Delaunay triangulation and Compact one (see Figure 6) [21].

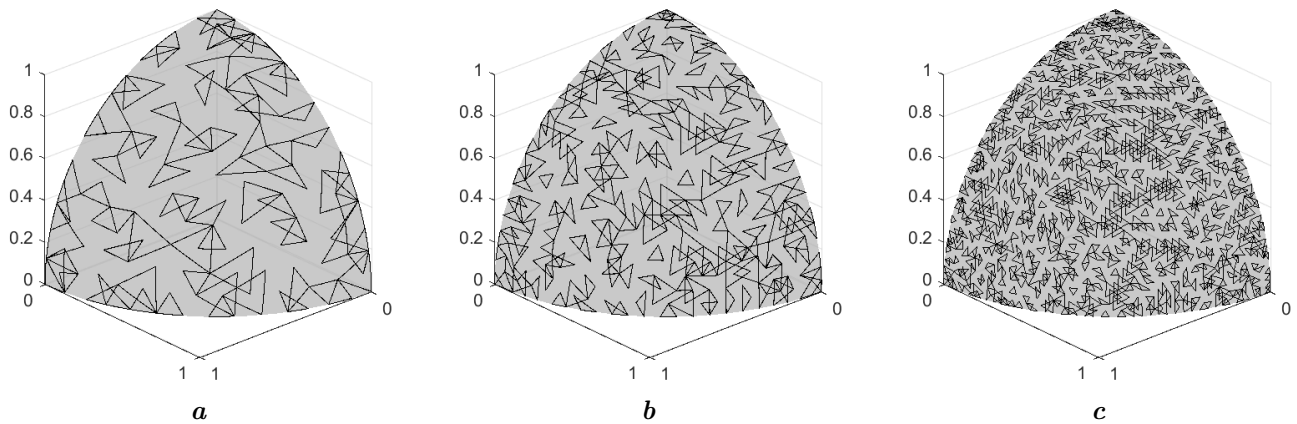


Fig. 4. Three of five Compact triangulations using: 146 points (a), 396 points (b), and 1512 points (c), corresponding to three sets of Figure 2.

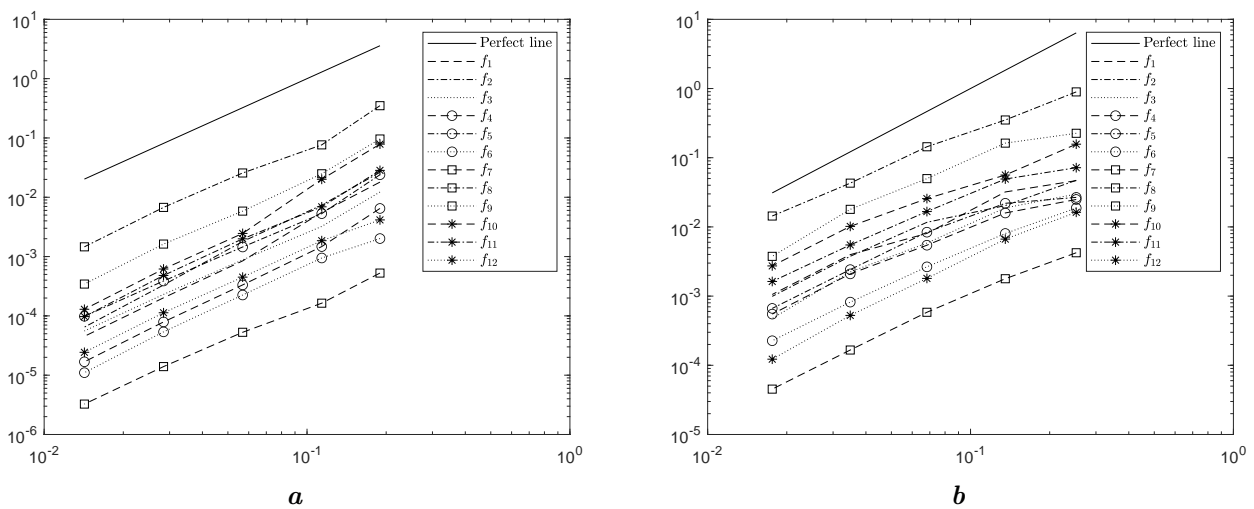


Fig. 5. Plot in logarithmic scale of the approximation error e_{\max} with respect to the maximum edge length h_{\max} for the operator K_2 applied to the 12 test functions using 184576 points, applying Delaunay triangulation (a), and Compact one (b).

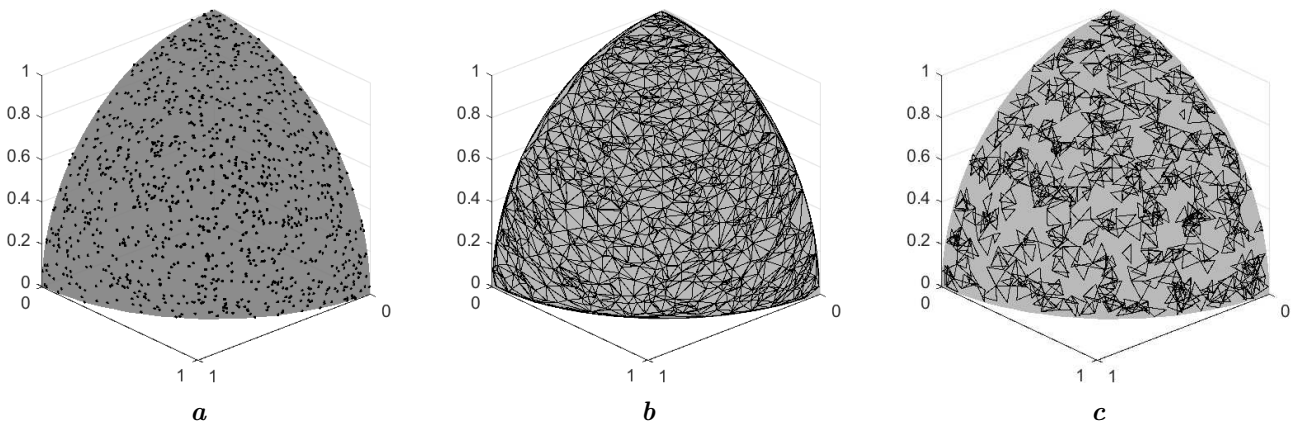


Fig. 6. Set of points on the sphere: 1119 points (a), Delaunay triangulation (2226 triangles) (b), and Compact triangulation (604 triangles) (c).

Table 3 presents the maximum error, mean average error, and square error (17). The errors $|S_2[f_i](\mathbf{u}) - f_i(\mathbf{u})|$ and $|K_2[f_i](\mathbf{u}) - f_i(\mathbf{u})|$ for $i = 1, \dots, 12$, are evaluated at 184576 points.

The obtained numerical results prove that the operators S_2 and K_2 have a signified accuracy specifically K_2 which is better than S_2 .

Table 3. Comparison between the operators S_2 and K_2 applied to 12 test functions, using the set of 1119 Halton points.

		$S_2[f]$	$K_2[f]$ Delaunay	$K_2[f]$ Compact
f_1	e_{\max}	1.2733e-01	9.4037e-03	3.1171e-02
	e_{mean}	9.7387e-03	3.0412e-04	7.0772e-04
	e_{MS}	1.7060e-02	7.7245e-04	1.9626e-03
f_2	e_{\max}	9.8447e-02	1.3097e-02	2.8714e-02
	e_{mean}	1.1497e-02	2.6833e-04	6.2748e-04
	e_{MS}	1.7675e-02	8.9528e-04	2.0609e-03
f_3	e_{\max}	1.2479e-01	1.2628e-02	2.7175e-02
	e_{mean}	1.4812e-02	3.5768e-04	8.2982e-04
	e_{MS}	2.2723e-02	7.7162e-04	1.7613e-03
f_4	e_{\max}	9.0704e-02	3.3433e-03	1.6352e-02
	e_{mean}	9.3213e-03	1.4731e-04	3.7152e-04
	e_{MS}	1.4659e-02	3.2256e-04	8.6497e-04
f_5	e_{\max}	2.9804e-01	2.2329e-02	4.1421e-02
	e_{mean}	1.9561e-02	3.0024e-04	8.0258e-04
	e_{MS}	2.8668e-02	6.4804e-04	1.5460e-03
f_6	e_{\max}	6.7440e-02	2.3250e-03	8.1282e-03
	e_{mean}	1.5168e-02	1.6535e-04	3.7932e-04
	e_{MS}	1.9008e-02	2.8684e-04	6.6235e-04
f_7	e_{\max}	4.4950e-02	1.6247e-03	2.5390e-03
	e_{mean}	6.2455e-03	4.7365e-05	1.2880e-04
	e_{MS}	8.2161e-03	9.5670e-05	2.2431e-04
f_8	e_{\max}	1.6181e+00	3.4981e-01	5.4937e-01
	e_{mean}	3.1255e-01	1.2262e-02	3.2284e-02
	e_{MS}	4.1255e-01	2.1566e-02	5.3857e-02
f_9	e_{\max}	6.0295e-01	7.5086e-02	1.0388e-01
	e_{mean}	1.1642e-01	3.6103e-03	8.4262e-03
	e_{MS}	1.5030e-01	6.3361e-03	1.3921e-02
f_{10}	e_{\max}	2.0805e-01	2.8305e-02	6.0498e-02
	e_{mean}	5.0055e-02	1.7609e-03	4.4316e-03
	e_{MS}	6.5143e-02	2.9785e-03	7.3068e-03
f_{11}	e_{\max}	2.8836e-01	3.7255e-02	9.3058e-02
	e_{mean}	4.2807e-02	1.4982e-03	3.7483e-03
	e_{MS}	6.1391e-02	2.6484e-03	6.4534e-03
f_{12}	e_{\max}	2.3407e-01	8.1012e-03	8.0565e-03
	e_{mean}	1.5786e-02	3.1086e-04	5.4027e-04
	e_{MS}	2.5275e-02	6.2016e-04	8.9395e-04

5. Conclusion and future works

This paper addressed the problem of interpolation of scattered data on the sphere. Here this kind of problem finds applications in many areas, including e.g. geophysics and meteorology. For this reason, there is a need for fast algorithms in order to interpolate large sets of scattered data.

In summary, this paper presents a powerful interpolation method to get an accurate functional approximation with less computational cost. This work will also be very helpful in many application fields, such as the numerical resolution of partial differential equations with new methods. Moreover, the proposed method is flexible, easily programmable, easily parallelizable, and completely automatic, since it works successfully even when the distribution of nodes is not uniform. This has been confirmed by a large number of numerical experiments.

In future, we will generalize and develop this study by working in a more general framework (a generalization to any Riemannian manifolds) and by presenting new triangulation strategies adapted

to this type of interpolation problem. Furthermore, this new interpolation strategy will be a strong point of the Shepard method, which would be an effective tool in many real applications, especially in space engineering, telecommunications, meteorology, astronomy, air quality, and air traffic.

-
- [1] Longman R. J., Frazier A. G., Newman A. J., Giambelluca T. W., Schanzenbach D., Kagawa-Viviani A., Needham H., Arnold J. R., Clark M. P. High-resolution gridded daily rainfall and temperature for the Hawaiian Islands (1990–2014). *Journal of Hydrometeorology*. **20** (3), 489–508 (2019).
 - [2] Maleika W. Inverse distance weighting method optimization in the process of digital terrain model creation based on data collected from a multibeam echosounder. *Applied Geomatics*. **12** (4), 397–407 (2020).
 - [3] Shepard D. A two-dimensional interpolation function for irregularly-spaced data. *Proceedings of the 1968 23rd ACM National Conference*. 517–524 (1968).
 - [4] Liszka T. An interpolation method for an irregular net of nodes. *International Journal for Numerical Methods in Engineering*. **20** (9), 1599–1612 (1984).
 - [5] McLain D. H. Drawing contours from arbitrary data points. *The Computer Journal*. **17** (48), 318–324 (1974).
 - [6] Farwig R. Rate of convergence of Shepard’s global interpolation formula. *Mathematics of Computation*. **46** (174), 577–590 (1986).
 - [7] Franke R., Nielson G. Smooth Interpolation of Large Sets of Scatter Data. *International Journal for Numerical Methods in Engineering*. **15** (11), 1691–1704 (1980).
 - [8] Renka R. J., Brown R. Algorithm 792: Accuracy Tests of ACM Algorithms for Interpolation of Scattered Data in the Plane. *ACM Transactions on Mathematical Software*. **25** (1), 78–94 (1999).
 - [9] Thacker W. L., Zhang J., Watson L. T., Birch J. B., Iyer M. A., Berry M. W. Algorithm 905: SHEPPACK: Modified Shepard algorithm for interpolation of scattered multivariate data. *ACM Transactions on Mathematical Software*. **37** (3), 1–20 (2010).
 - [10] Karandashev K., Vaníček J. A combined on-the-fly/interpolation procedure for evaluating energy values needed in molecular simulations. *The Journal of Chemical Physics*. **151** (17), 174116 (2019).
 - [11] Farrahi G. H., Faghidian S. A., Smith D. J. An inverse approach to determination of residual stresses induced by shot peening in round bars. *International Journal of Mechanical Sciences*. **51** (9-10), 726–731 (2009).
 - [12] Alfeld P., Neamtu M., Schumaker L. L. Fitting scattered data on sphere-like surfaces using spherical splines. *Journal of Computational and Applied Mathematics*. **73** (1–2), 5–43 (1996).
 - [13] Baramidze V., Lai M., Shum C. K. Spherical splines for data interpolation and fitting. *SIAM Journal on Scientific Computing*. **28** (1), 241–259 (2006).
 - [14] Cavoretto R., De Rossi A. A spherical interpolation algorithm using zonal basis functions. *International Conference on Computational and Mathematical Methods in Science and Engineering (CMMSE09)*. **1**, 258–269 (2009).
 - [15] Fasshauer G. E. Adaptive least squares fitting with radial basis functions on the sphere. *Mathematical methods for curves and surfaces*. 141–150 (1995).
 - [16] Fasshauer G. E., Schumaker L. L. Scattered data fitting on the sphere. *Mathematical Methods for Curves and Surfaces II*. 117–166 (1998).
 - [17] Meyling R. G., Pfluger P. R. B-spline approximation of a closed surface. *IMA Journal of Numerical Analysis*. **7** (1), 73–96 (1987).
 - [18] Pottmann H., Eck M. Modified multiquadric methods for scattered data interpolation over a sphere. *Computer Aided Geometric Design*. **7** (1–4), 313–321 (1990).
 - [19] Sloan I. H., Womersley R. S. Constructive polynomial approximation on the sphere. *Journal of Approximation Theory*. **103** (1), 91–118 (2000).
 - [20] Womersley R. S., Sloan I. H. How good can polynomial interpolation on the sphere be? *Advances in Computational Mathematics*. **14** (3), 195–226 (2001).
 - [21] Dell’Accio F., Di Tommaso F., Hormann K. On the approximation order of triangular Shepard interpolation. *IMA Journal of Numerical Analysis*. **36**, 359–379 (2016).

- [22] Horemuž M., Andersson J. V. Polynomial interpolation of GPS satellite coordinates. *GPS Solutions*. **10**, 67–72 (2006).
- [23] Coxeter H. S. M., Greitzer S. L. *Geometry revisited*. Mathematical Association of America. **19** (1967).
- [24] Dell’Accio F., Di Tommaso F., Nouisser O., Zerroudi B. Fast and accurate scattered Hermite interpolation by triangular Shepard operators. *Journal of Computational and Applied Mathematics*. **382**, 113092 (2021).
- [25] Langer T., Belyaev A., Seidel H. P. Spherical barycentric coordinates. *Symposium on Geometry Processing* (2006).
- [26] Königsberger K. *Analysis 2*. Springer-Verlag (2013).
- [27] Renka R. J. Multivariate interpolation of large sets of scattered data. *ACM Transactions on Mathematical Software (TOMS)*. **14** (2), 139–148 (1988).
- [28] Hubbert S., Morton T. M. L_p -error estimates for radial basis function interpolation on the sphere. *Journal of Approximation Theory*. **129**, 58–77 (2004).
- [29] Nouisser O., Zerroudi B. Modified Shepard’s method by six-points local interpolant. *Journal of Applied Mathematics and Computing*. **65**, 651–667 (2021).
- [30] Richard F. Scattered data interpolation: Tests of some methods. *Mathematics of Computation*. **38** (157), 181–200 (1982).

Ефективна інтерполяція розсіяних даних на сфері методом Шепарда

Зерроді Б.¹, Тайек Х.^{2,3}, Ель Харрак А.³

¹Лабораторія інженерних наук, Факультет природничих наук, Університет Ібн Зор Агадір, Марокко

²SMAD, FPL, Університет Абдельмалека Ессааді, Тетуан, Марокко

³ММА, FPL, Університет Абдельмалека Ессааді, Тетуан, Марокко

У статті представлено два оператори апроксимації великих розсіяних наборів даних для сферичної інтерполяції. Запропонований метод розв’язання є розширенням добре відомого методу сферичної інтерполяції Шепарда, який використовує інвертовані відстані розсіяних точок як вагові функції. У зв’язку з цим перший запропонований оператор є лінійною комбінацією базисних функцій, коефіцієнти яких є значеннями функції. Що стосується другого оператора, то розглянуто сферичну триангуляцію розсіяних точок і замінено значення функції на локальний інтерполянт, який локально інтерполірує задані дані у вершинах кожного трикутника. Крім того, були проведені чисельні тести для демонстрації ефективності інтерполяції, де декілька чисельних результатів виявляють значну точність наближення запропонованих операторів.

Ключові слова: сферичне наближення; сферичні RBFs; модифікований метод Шепарда; барицентричні координати.